A neutron radiation-hardened superluminescent diode

Jiao Jian(焦健)[1, †], Tan Manqing(谭满清)[1], Zhao Miao(赵妙)[1, 2], and Chang Jinlong(常金龙)[1]

[1] Institute of Semiconductors, Chinese Academy of Sciences, Beijing 100083, China
[2] Institute of Microelectronics, Chinese Academy of Sciences, Beijing 100029, China

Abstract: We present a novel superluminescent diode (SLD) with high optical performances for hardened neutron irradiation. The degradation of the light output from the SLDs is caused by a reduction of the minority carrier lifetime resulting from displacement damage after high-energy neutron irradiation. The SLDs with a higher pre-irradiation light output will be less sensitive to radiation. We have selected an InGaAsP/InP multi-quantum well (MQW) as the active region structure for its performance, its high optical gain and minute active region. Graded-index separate-confinement-heterostructure (GRIN-SCH) has been applied for the waveguide structure. A specific absorbing region and anti-reflective coatings have been designed and optimized. Moreover, the radiation test results indicate that the SLD with an InGaAsP/InP MQW structure has better neutron hardening ability than the SLD with DH structures after a 6×10^{13}–1×10^{14} n/cm^2 1 MeV neutron irradiation.

Key words: superluminescent diode; neutron irradiation; InGaAsP/InP multi-quantum well
DOI: 10.1088/1674-4926/33/9/094006 **PACC:** 6180H

1. Introduction

The fibre optic gyroscope (FOG) is one kind of optical fiber sensor based on the Sagnac effect that uses the interference of light to detect mechanical rotation. In the past 20 years, FOG has been become the leading gyroscope, with solid-state structure, large dynamic-range, low power consumption, high reliability and low cost etc, while it can serve the purpose of satellite attitude control, with the development of gyroscopic technologies. As the most important light source in the FOG, a superluminescent diode (SLD) will be used in space systems and nuclear explosions. It is well known, however, that the radiation exposure containing neutron irradiation in a bad environment can be detrimental to the photoelectric diodes. Therefore, it is required to study the neutron irradiation effects in the SLD under a space radiation environment, based on the research of neutron-irradiation induced optical property changes in the LD and LED[4−9], including exploring the physics mechanism of SLD degradation, confirming the irradiation sensitivity parameter, which have not been studied yet at home and abroad and will provide the foundation for radiation hardening design.

In this paper, the effects caused by neutron irradiation in the SLD and the methods of neutron hardening for the device are represented. Through academic analysis, calculations and simulative experiments, the InGaAsP/InP multi-quantum well (MQW) active region and graded-index separate-confinement-heterostructure (GRIN-SCH) waveguide have been applied for the epitaxial structure of the neutron radiation-hardened SLD. A specific waveguide structure for lasing suppression has also been designed and optimized. Both the hardened and unhardened SLDs are irradiated by the nuclear reactor at the Northwest Institute of Nuclear Technology, under 6×10^{13}–1×10^{14} n/cm^2 1 MeV neutron irradiation. The results show that the SLD with InGaAsP/InP MQW structures have better neutron fluence immunity than the SLD with DH structures.

2. Neutron radiation effects in a superluminescent diode[1−3]

The damage caused by high-energy neutron irradiation in the SLDs is mainly due to lattice displacements, while negligible ionization damage occurs. Displacement damage can have a significant impact on their optical properties, through the creation of stable radiation defects, which have one or more levels in the bandgap. Important material parameters such as carrier mobility and density, generation (τ_g) and recombination (τ_r) lifetimes will be affected. First, the removal or reduction of the free carriers occurs due to direct removal of dopants from substitutional lattice sites by interaction with the created vacancies and interstices giving rise to stable point defects. Furthermore, non-radiative recombination centers that compete with radiative centers for excess carriers are created by radiation-induced deep level defects, which results in a decrease of the minority carrier lifetime τ. The reciprocal of the minority carrier lifetime degrades linearly with fluence Φ, but the constant of proportionality (the damage constant K) depends on particle type and energy. Lifetime damage can be described by[6]

$$\tau_0/\tau = 1 + \tau_0 K \Phi. \quad (1)$$

The ratio of the pre-irradiation (P_0) and post-irradiation (P_Φ) light output is given by[6]

$$(P_0/P_\Phi)^{2/3} - 1 = \tau_0 K \Phi, \quad (2)$$

where τ_0 and τ are the minority carrier lifetimes before and after exposure to a radiation dose or fluence Φ. K is a damage constant which depends on the interaction between semiconductor material and radiation field. The minority carrier lifetime will decrease when the product $\tau_0 K \Phi$ is compared to 1, and leads to a reduction in light output, from which readily follows that the larger the product $\tau_0 K$ (as a relative measure of

† Corresponding author. Email: jiaojian@semi.ac.cn
Received 5 March 2012, revised manuscript received 10 April 2012

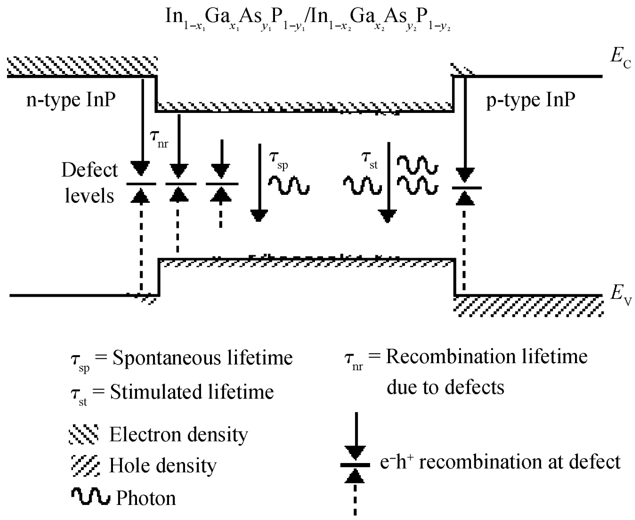

Fig. 1. Competitive mechanism between the radiative recombination and nonradiative recombination in an InGaAsP/InP SLD.

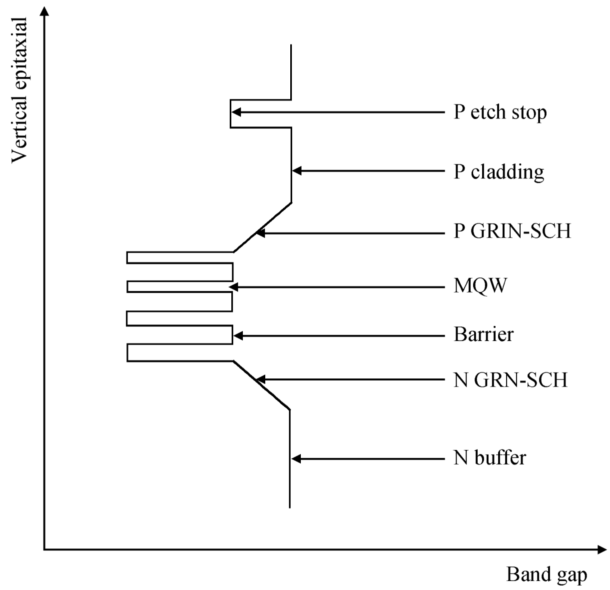

Fig. 2. Epitaxial structure versus band gap of non-uniform well thickness MQWs[11].

damage), the more prone the SLDs will be to radiation damage. Reducing the value of $\tau_0 K$ can be achieved by minimizing the pre-irradiation lifetime τ_0.

Figure 1 shows that the process of the radiative recombination and non-radiative recombination are in competition, when an InGaAsP/InP SLD is charged by the forward injection current after fast neutron irradiation.

$$R = R_r + R_i + R_A, \tag{3}$$

where R is represented as the total recombination rate, consists of the radiative recombination rate as R_r, nonradiative recombination rate as R_i and Auger recombination rate as R_A. Recombination rate is the reciprocal of carrier lifetime, so the total carrier recombination lifetime τ can be expressed as

$$\frac{1}{\tau} = \frac{1}{\tau_r} + \frac{1}{\tau_i} + \frac{1}{\tau_A}, \tag{4}$$

where τ_r , τ_i and τ_A are called the radiative recombination lifetime, non-radiative recombination lifetime and Auger recombination lifetime, respectively. Quantum efficiency (η_i') is the ratio of the radiative recombination rate (R_r) and total recombination rate (R) light output, which is given by

$$\eta_i' = \frac{R_r}{R} = \frac{\tau}{\tau_r}, \tag{5}$$

$$\eta_i' = \frac{\tau_i \tau_A}{\tau_i \tau_A + \tau_r \tau_A + \tau_r \tau_i}. \tag{6}$$

Equations (5) and (6) indicate that the device with the higher quantum efficiency will have shorter radiative recombination lifetime τ_r which here represents the pre-irradiation lifetime τ_0. The device then will have high pre-irradiation light output due to a small τ_0, and will also be less sensitive to neutron irradiation. Therefore, the most effective method to improve the neutron hardening ability is to design a kind of SLD with high quantum efficiency.

As a kind of light amplifying incoherent light source by spontaneous emission, an SLD module is ideal for military fibre optic gyroscopes because of a high light output, wide spectrum bandwidth and low ripple factor. It consists of a superluminescent LED, a thermistor, a Peltier cooler (TEC) and a polarization maintaining fiber (PMF). Displacement damages can be easily caused in each unit of the SLD module, another effective method for neutron hardening is thus taken to making a novel uncooled SLD, where a superluminescent LED can still remain a stable working state without the thermistor and TEC, which needs us to design an active region structure with a lower temperature sensitivity (a higher characteristic temperature). What is also needed is a low volume active region, having the same effect of decreasing neutron radiation sensitivity, which can reduce the displacement damages in the light emission area as much as possible.

3. Design and implementation of a neutron radiation-hardened superluminescent diode

3.1. Epitaxial structure design

It is known that a neutron radiation-hardened superluminescent diode must have high quantum efficiency and a minute active region, both of which the InGaAsP/InP multi-quantum well (MQW) structures have, compared with the double heterojunction (DH) structures[3]. The research on the InGaAsP/InP MQW active region structure and the effect of thickness, QW shape, doping and composition on SLD performance are involved in our work on epitaxial structure design and optical performance of the neutron radiation-hardened SLD.

In order to achieve a high light output, wide spectrum width and low ripple factor, we have selected 4 InGaAsP/InP MQWs with non-uniform well widths of 6 nm, 6 nm, 8 nm and 8 nm as the active region structure of the neutron radiation-hardened SLD, as shown in Fig. 2. Graded-index separate-confinement-heterostructure (GRIN-SCH) has been applied for the designed waveguide structure. The active layer consists of four non-uniform thicknesses of $In_{1-x}Ga_xAs_yP_{1-y}$ MQWs with the quantized energies corresponding to 1310 nm, sepa-

Table 1. Epitaxial structure of 1310 nm neutron radiation-hardened SLD.

Layer name		Material	Doping and type (cm^{-3})
P contact		InGaAs	$P = 3.5 \times 10^{19}$
P upper cladding		InP	$P = 2 \times 10^{18}$
P etch stop		InGaAsP	$P = 2 \times 10^{18}$
P cladding		InP	$P = 2 \times 10^{18}$
P GRIN-SCH		$InGa_xAs_yP$ ($x = 0.3$–0.45, $y = 0.8$–0.65)	$P = 1 \times 10^{17}$
MQWs active	3 barriers	InP	Undoped
MQWs active	4 wells	$In_{1-x}Ga_xAs_yP_{1-y}$ ($\lambda = 1310$ nm)	Undoped
N GRIN-SCH		$InGa_xAs_yP$ ($x = 0.45$–0.3, $y = 0.65$–0.8)	$N = 1 \times 10^{17}$
N buffer		InP	$N = 3.5 \times 10^{18}$
Sub		InP	

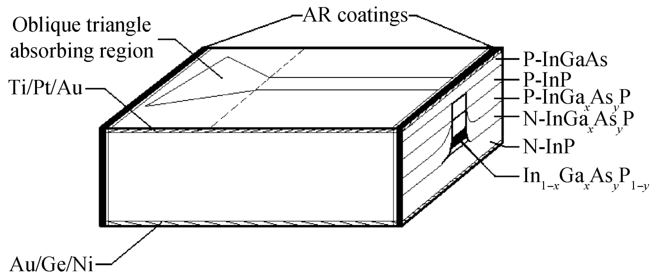

Fig. 3. Schematic structure of the InGaAsP/InP MQWs SLD.

rated by three 10-nm-thick lattice matched InP barriers. A linearly variable $InGa_xAs_yP$ structure is used on both sides of the active region as the GRIN-SCH layer. Then a p-InP cladding layer and a p-InGaAsP etch stop layer are grown on the p-GRIN-SCH layer. The thicknesses of the GRIN-SCH layer and the cladding layer are optimized to expand the mode in the transverse direction for the sake of improving the coupling efficiency of 1310 nm SLD. Finally, a p-InP upper cladding layer and a p-InGaAs contact layer are grown to embed these layers completely. The detailed epitaxial structure of a 1310 nm neutron radiation-hardened SLD is shown in Table 1.

We also design a new kind of oblique triangle structure for the absorbing region, combined with a two layer structure for anti-reflective coating. The characteristics of the oblique triangle absorbing region is that it has a particular included angle of 3–20 degrees between each edge and its corresponding cavity surface, which can effectively increase the light transmittance. A two layer structure of AR coating has a better advantage not only on the spectral region bandwidth with low reflectivity but also on the influence of the refractive index and the thickness deviation of film material on the residual reflectivity of the film system. The reflectivity from facets of the SLDs can be reduced by preparing this specific waveguide structure and evaporating AR coatings on facets. It is found that the damage caused by neutron irradiation can be effectively reduced and a relatively high output power can be obtained through simulation and calculations when the absorbing region is 150 μm with a whole cavity length of 500 μm. Finally, the schematic structure of the InGaAsP/InP MQWs SLD is shown in Fig. 3.

3.2. Device implementation

First, InGaAsP/InP MQW active region structures are fabricated on an InP substrate by metal-organic chemical vapor deposition (MOVCD). After a SiO_2 film is coated by plasma-enhanced chemical vapor deposition (PECVD) on the active structure, the designed mask pattern is printed on the film by photolithography, then GRIN-SCH waveguide structures are obtained through wet etching, with n-InP and p-InP cladding layers grown on successively. The mask on the p-GRIN-SCH layer, on which the upper cladding layer reach the same mesa is then etched. The absorbing region is prepared after a SiO_2 mask is coated on the high doping p-InGaAs contact layer. Then, Ti/Pt/Au is coated on the P side and Au/Ge/Ni is coated on the N side after thinning. Finally, AR coatings on two end faces of the SLDs are prepared by the technology of high vacuum electron-beam evaporation. Thus, the whole structure of a neutron radiation-hardened SLD is successfully implemented.

4. Radiation test results and analysis

We fabricate two different kinds of SLDs as radiation samples: one is the neutron radiation-hardened SLD with InGaAsP/InP MQW structures, the other is the unhardened with DH structures. Both of them are irradiated by the nuclear reactor at the Northwest Institute of Nuclear Technology. The neutron fluence ranges from 6×10^{13} n/cm^2 to 1×10^{14} n/cm^2 (fast neutron energy = 1 MeV, $n/\gamma = 6.1 \times 10^9$ n/rad (Si)).

Considering the neutron irradiation protection problem, our method for this experiment is the static shift test, moving the unbiased samples away from the neutron irradiation position then doing the photoelectric parameters test. P–I and I–V characteristics of all the samples are measured by a P–I–V testing system, while spectral characteristics containing center wavelength and spectrum width are measured by spectrometer at room temperature, before the experiment began and after a neutron dose of the samples came down to the allowable value, respectively.

4.1. Light output characteristics

Figure 4 shows the decrease in light output of MQW and DH at 18 ℃ as a function of neutron irradiation. We find that

Table 2. Center wavelength and spectrum width of the SLDs before and after neutron irradiation.

Sample	Neutron fluence (n/cm^2)	Center wavelength (nm)		Spectrum width (nm)	
		Before irradiation	After irradiation	Before irradiation	After irradiation
MQW1	1×10^{14}	1304	1304	56.2	55.6
MQW2	1×10^{14}	1307	1307	55.3	54.9
DH1	1×10^{14}	1291	1291	45.6	44.7
DH2	1×10^{14}	1291	1291	44.7	44.6

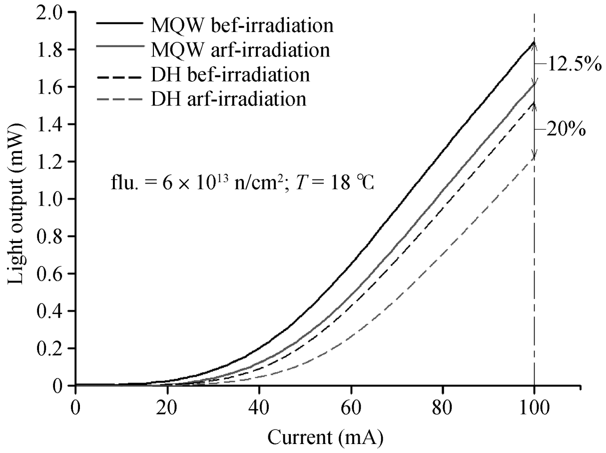

Fig. 4. P–I curves of MQW and DH before and after neutron irradiation.

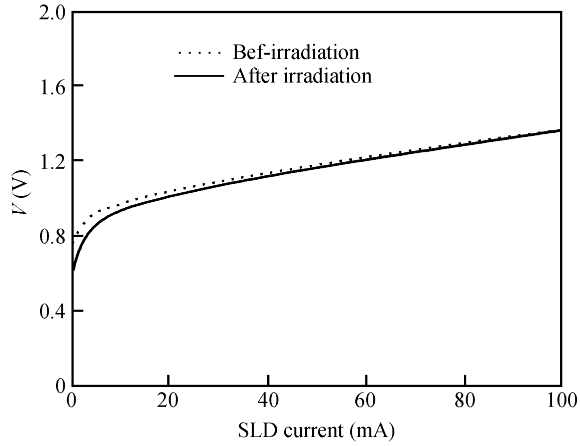

Fig. 6. I–V characteristics of MQW before and after neutron irradiation ($\Phi = 1 \times 10^{14}$ n/cm^2, $T = 25$ ℃).

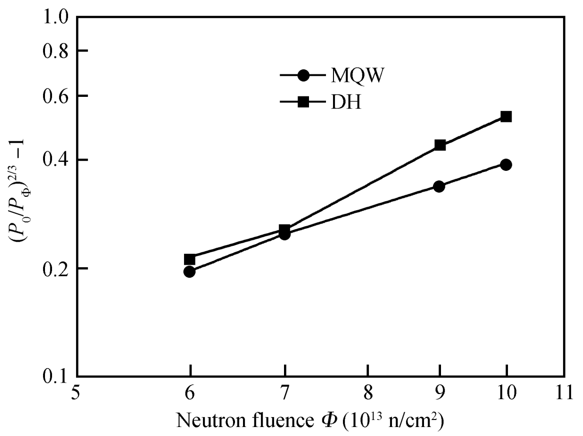

Fig. 5. $(P_0/P_\Phi)^{2/3} - 1$ versus Φ curve of MQW and DH before and after the neutron irradiation at 18 ℃.

the light output of MQW decreased to 12.5% under a working current of 100 mA in a temperature-controlled environment, while a reduction of DH's light output by ~20% under the same 6×10^{13} n/cm^2 neutron irradiation.

From Eq. (2) it readily follows that $\tau_0 K$ is the slope value if the $(P_0/P_\Phi)^{2/3}-1$ versus Φ curve in the range of 6×10^{13}–1×10^{14} n/cm^2 has a good linear relationship. As an important measure of radiation damage, the smaller the value of $\tau_0 K$, the less sensitive the SLD will be to radiation damage. Figure 5 shows the linear relationship between $(P_0/P_\Phi)^{2/3} - 1$ and Φ of MQW and DH before and after neutron irradiation. By using the Origin fitting method, we find that the $\tau_0 K$ of MQW is about 1.34, less than about 2.05 of DH, which thus explains why the SLD with InGaAsP/InP MQW structures has less output decay than the SLD with DH structures.

Due to exponential dependence of SLD optical power on gain, the change of SLD power strongly depends on temperature variations. Without temperature control, a temperature rise caused by cumulative thermal effects results in not only the increase of the internal loss coefficient, carrier leakage losses and internal losses, but also the reduction of the internal quantum efficiency, which causes the threshold current density to gradually increase. This will be the second reason for the degradation of output power, compared with the impact of the displacement damage on the output power. Therefore, it is necessary to measure the light output in a temperature-controlled environment to reduce the errors in a neutron irradiation experiment.

4.2. I–V characteristics

Figure 6 shows current I versus voltage V characteristics of MQW at 25 ℃ before and after neutron irradiation. We find that the forward I–V is modified by 1×10^{14} n/cm^2 irradiation, with a shift of current towards higher values, which indicates the creation of an excess space change recombination current component caused by non-radiative recombination centers. As the working current increases, the radiation damage can be partly removed by a large forward current either during or after the irradiation[12]. The more the current injects the less sensitive the device will be to radiation damage. To a large extent, the defect annealing may be related to self-heating.

4.3. Spectral characteristics

Table 2 shows that after neutron irradiation, the center wavelength of the SLDs remain the same, which indicates that no thermal effect is induced by neutron irradiation. On the other hand, the greatest change of spectrum width is only 0.9nm in the range of measuring errors. It seems that the neutron fluence is not strong enough to affect the spectral characteristics of the SLDs.

5. Conclusions

A novel neutron radiation-hardened SLD with high optical performance has been designed and implemented. In order to achieve high light output, wide spectrum width and low ripple factor, an InGaAsP/InP multi-quantum well and graded-index separate-confinement-hetero structure have been applied to the wafer structure of the neutron radiation-hardened SLD, as the active region structure and the waveguide structure, respectively. We also design a new kind of oblique triangle structure for the absorbing region, combined with a two-layer structure for anti-reflective coatings. The samples of hardened and unhardened SLDs are irradiated by the nuclear reactor at the Northwest Institute of Nuclear Technology. The radiation test results show that the SLD with InGaAsP/InP MQW structures, which is more suitable for space applications, has less output decay than the SLD with a DH structures after a 6×10^{13}–1×10^{14} n/cm^2 1 MeV neutron irradiation. A small increase in current has been observed, but spectral characteristics remain the same as before the neutron irradiation.

References

[1] Lin Libin. Introduction of radiation solid physics. Chengdu: Sichuan Publishing House of Science and Technology, 2004

[2] Chen Panxun. Radiation effect in semiconductor devices and integrated circuits. Beijing: National Defence Industrial Press, 2005

[3] Jiang Jiangping. Semiconductor lasers. Beijing: Publishing House of Electronics Industry, 2000

[4] Carson R F, Chow W W. Neutron effects in high-power GaAs laser diodes. IEEE Trans Nucl Sci, 1989, 36: 2076

[5] Rudenko N M, Kuzmenko O M. The influence of neutron radiation on characteristics of the LED with red and yellow emission color. TCSET, Lviv-Slavske, Ukraine, 2010

[6] Lischka H, Henschel H, Kohn O, et al. Radiation effects in light emitting diodes, laser diodes, photodiodes and optocouplers. The IEEE Proc RADECS, New York, 1994: 226

[7] Ohyama H, Simoen E, Claeys C, et al. Radiation-induced lattice defects in InGaAsP laser diodes and their effects on device performance. Physica B, 1999, 273/274: 1031

[8] Ohyama H, Simoen E, Claeys C, et al. Impact of neutron irradiation on optical performance of InGaAsP laser diodes. Thin Solid Films, 2000, 364: 259

[9] Johnston A H. Radiation effects in light-emitting and laser diodes. IEEE Trans Nucl Sci, 2003, 50(3): 689

[10] Mudron J, Mullerova J, Dubecky F. Optical properties of semi-insulating GaAs irradiated by neutrons. Solid-State Electron, 1998, 42: 243

[11] Minch J. Theory and experiment of $In_{1-x}Ga_xAs_yP_{1-y}$ and $In_{1-x-y}Ga_xAl_yAs$ long-wavelength strained quantum-well lasers. IEEE J Quantum Electron, 1999, 35(5): 771

[12] Barnes C E. A comparison of gamma-irradiation-induced degradation in amphoterically Si-doped GaAs LED's and Zn-diffused GaAs LED's. IEEE Trans Electron Devices, 1979, 26: 739